Bulgarian Chemical Communications, Volume 50, Special Issue L (pp. 139 – 146) 2018

Prevent of greenhouse gas emissions in aluminum smelter by carbon nanotube (Monte Carlo simulation)

M .Ameri Siahooei, Kh. Mehrani*, M.Yousefi
[1]*Department of chemistry, Science and Research branch, Islamic Azad University, Tehran, Iran.*

Submitted March 24, 2016; Accepted August 8, 2016

Greenhouse gas emissions in aluminum smelter and separation this gases from hydrogen is very important. The gaseous constituents are carbon dioxide, sulphur dioxide and hydrogen fluoride , carbon tetrafluoride, di-carbon hexa-fluoride, silicon tetrafluoride, hydrogen sulphide, carbon disulphide, and hydrocarbons gaseous have been identified. Challenged by growing environmental concerns, the primary aluminium industry has undergone major changes over the last two decades to become a much more efficient industry with GHG emissions during the smelting process. The aluminium indndustry has been identified as a major contributor to GHG emissions and is therefore under particular scrutiny from the Intergovernmental Panel on Climate Change (IPCC), one of whose targets is to reduce these emissions by 50 to 85% by2050.This study has been conducted to figure out the adsorption and separation of greenhouse gas emissions with hydrogen on (8,8) armchair carbon nanotubes (CNTs). Lennard-Jones potential was used for gas-gas and gas-carbon nanotube interactions and the potential parameters for the carbon-gas and carbon-carbon interactions were obtained from the Lorenz-Berthelot combining rules. My calculations have shown that adsorption between hydrogen and these gases in aluminum smelter is possible and separation between studied gases in inside and first layer of outside carbon nanotube is possible

Keywords: “carbon nanotube, monte carlo simulation,adsorption gas”

INTRODUCTION

Greenhouse gas emissions in the production of primary aluminum come from processes such as coke calcination, anode production and consumption, lime production, and electrical generation. Process carbon dioxide emissions make up about half of total direct carbon dioxide equivalent emissions from aluminum production with the remaining greenhouse gases (GHG) emitted being perfluorinated carbon (PFC) gases. For example, the measurements of the two perfluorocarbons (PFCs) tetrafluoromethane (CF4) and hexafluoroethane (C2F6) -- emitted directly from the manufacture of primary aluminum are used in the calculation of facility specific greenhouse gas emission factors. Commercial aluminum production has been identified as the largest emitter of these two compounds. Although the annual amount of PFC emissions is not great, the impact is magnified because of the high global warming potentials (GWPs) of these two gases over the lifetime of the a facility**.**

Fluoride emissions in the form of gaseous hydrogen fluoride and sodium and aluminium fluorides and unused cryolite as particulates, are the major undesirable fume component produced in the aluminium smelting process. Such emissions can be reduced through the use of fume control systems, operational good practice and improved technology.. The gaseous fluorides generated in the process are mainly HF, CF_4, C_2F_6 and SiF_4, the major component being HF. The particulates are mainly mixtures of aluminum oxides and cryolite [1]. This paper focuses on the Prevention globalwarming potential (GWP) in primary aluminum production and the aim of this paper is this problem. Figure 1 and 2 show that emissions fluoride increasing by increase the production of aluminum [2].

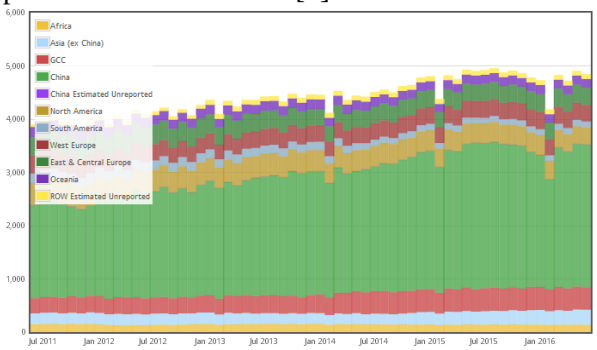

Fig. 1. Total for Jun 2011 to Jun 2016: 269,050 thousand metric tonnes of aluminium

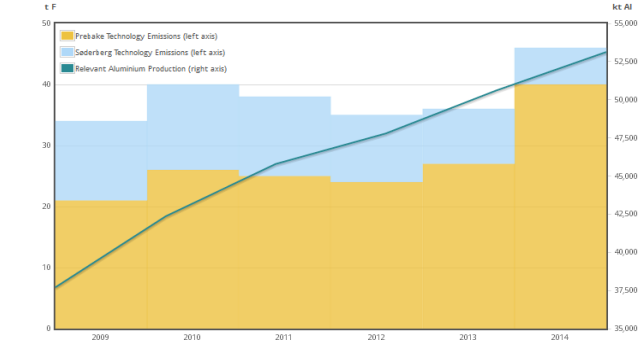

Fig. 2. Generation of unwanted fluoride by-products from the aluminium smelting

* To whom all correspondence should be sent:
E-mail: Kh.mehrani@gmail.com

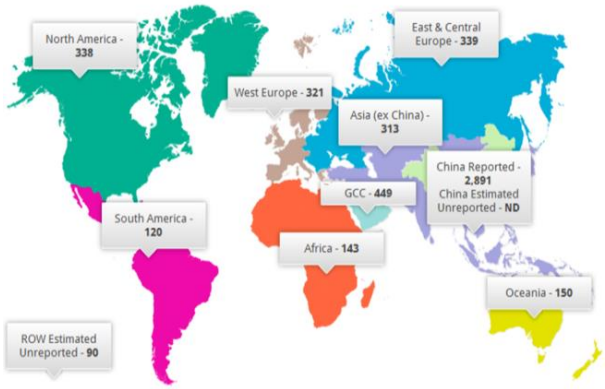

Fig. 3. Total for Dec 2016: 5,154 thousand metric tonnes of aluminium

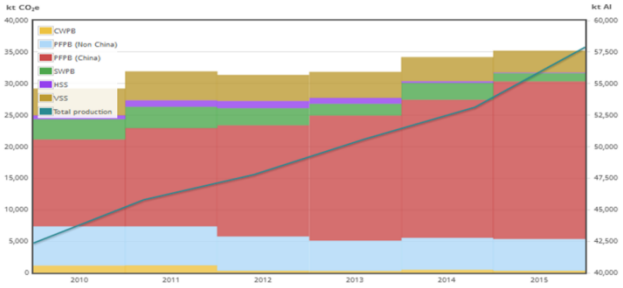

Fig. 4. Global PFC Emissions for 2010 to 2015 in kt CO_2e from the aluminium smelting

Sears et al. [3] study on carbon nanotubes (CNTs) are nanoscale cylinders of graphene with exceptional properties such as high mechanical strength, high aspect ratio and large specific surface area. To exploit these properties for membranes, macroscopic structures need to be designed with controlled porosity and pore size.

Nickmand et al. [4] study on Grand canonical Monte Carlo (GCMC) simulation is usedto model adsorption of CO2 and SO2 molecules by the pure and functionalized single walled carbon nanotubes(SWCNT and FSWCNT). Simulations are conducted for two cases: i) Without and ii) with a 5.75Å clearance between the CNT wall and the walls of the simulation box. Results show that the adsorption capacity for the SO2 molecules is generally higher than that of the CO2 molecules, especially at low pressures [4].

Gatica & Nekhai [5] in Department of Physics and Astronomy, Howard University,study on Monte Carlo simulations of the adsorption of neon, argon, methane and carbon dioxide in carbon nanohorns. They model the nanohorns as an array of carbon cones and obtained adsorption isotherms and isosteric heats. The main sites of adsorption are inside the cones and in the interstices between three cones. They also calculated the selectivity of carbon dioxide/methane, finding that nanohorns are a suitable substrate for gas separation.

In this work, grand canonical Monte Carlo (GCMC) method is used to study the compounds adsorption gas on carbon nanotube. Single-Walled carbon nanotubes are selected to be the adsorbent. To make a comprehensive work, the influence of temperature as well as pressures on the adsorption is also studied.

The simulation results in this work can be used to optimize the separation between hydrogen and Fluoride Gases in aluminum smelter at a given pressures and temperatures.

We published an article dedicated to nano-technology to remove toxic h_2s gaseous compounds from exhaust gases in primary aluminum industry [6]. Given the importance of adsorption and separation and adsorption of these gases in aluminum industry this project in the after it was defined.

SIMULATION METHOD

The Monte carlo statistical mechanical simulation were carried out in standard manner using the Metropolis sampling technique in canonical *(T, V, N)* ensamble. In this work, all of the particles include Sulfur compounds molecules, and carbon atoms are treated as structureless spheres. Particle-Particle interactions between them are modeled with Lennard-Jones potential located at the mass-center of the particles. In this work, as in the works of many researchers, the cut and shifted Lennard-Jone (LJ) potential was used to represent the interaction between HF, CF_4, C_2F_6 and SiF_4 compounds molecules.

$$\phi_{ff}(r)=\begin{cases}\phi_{ij}(r)-\phi_{ij}(r_c) & r<r_c\\ 0 & r\geq r_c\end{cases} \quad (1)$$

Where r is the interparticle distance, r_c is the cut off radius, $r_c = 5\sigma_{ff}$. ϕ_{ij} is the full LJ potential, $\phi_{ij}=4\varepsilon_{ff}\left[\left(\sigma_{ff}/r\right)^{12}-\left(\sigma_{ff}/r\right)^{6}\right]$, where ε_{ff} and δ_{ff} are the energy and size parameters of the fluid .They are 301.1 and 3.62nm for hydrogen sulfide also 335.4 and 4.112nm for Sulfur dioxide also 467 and 4.483 for Carbon disulfide here [5-7].

The interaction between the wall and a hydrogen sulfide molecule is calculated by the site-to-site method[8,9].

$$U_{fw}=4\varepsilon_{fw}\sum_{i=1}^{N_f}\sum_{j=1}^{Ncabon}\left[\left(\frac{\sigma_{fw}}{r_{ij}}\right)^{12}-\left(\frac{\sigma_{fw}}{r_{ij}}\right)^{6}\right] \quad (2)$$

For example Where N_f is the number of Sulfur dioxide gas molecules, N_{carbon} is the number of carbon atoms of the wall of SWNT ε_{fw} and δ_{fw}. are

the cross-energy and size parameters, which are obtained from the Lorentz-Berthelot (LB) combining rules. Energy and size parameters of carbon atoms are 28.0 and 0.34nm, respectively [10].

The quantity r_{ij} is the distance between a gas hydrogen sulfide molecule and an atom of the wall of SWNT.

Lorentz-Berthelot rules are used to calculate the parameters of interaction between different kinds of particles.In this calculation, all of the particles are regarded as spheres. Interaction among particles are modeled with Lennard-Jones potential acted on the mass center. The initial configuration was generated randomly (Figure1). For a fixed cell, three types of moves were used to generate a markov chain, including moving, creating, and deleting a molecule and make new configurations. The three types of moves have the same probability and each has different receiving opportunities. Configurations are accepted when they obey Metropolis's Sampling scheme in proportion to exp (*-Ea/RT*) where ΔE is the change of total energy in the system.

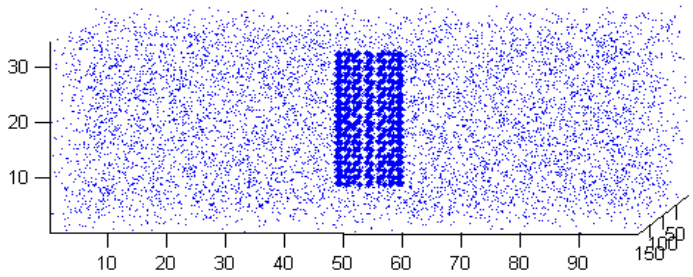

Fig. 5. .Initial configuration

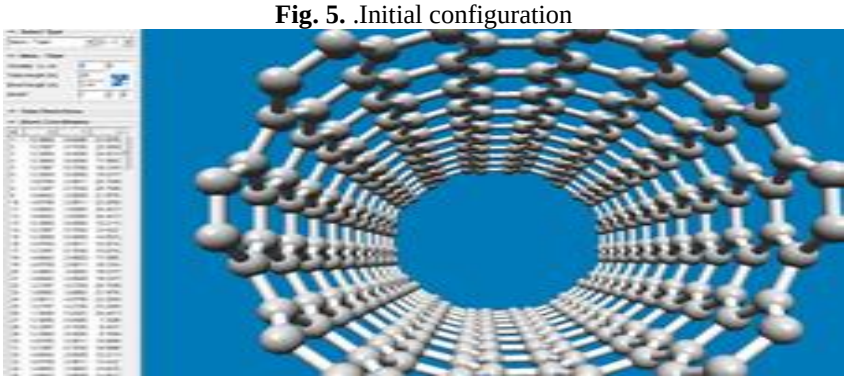

Fig. 6. Armchiar (8,8)

To insure good thermodynamical averages, for a single isotherm point typically 5×10^6 moves have been performed to equilibrate the system. for each of five hundred configuration, one configuration is selected, and names snapshot. diagram energy of produced configuration to namber of snapshot show that system reach to the equilibrium.

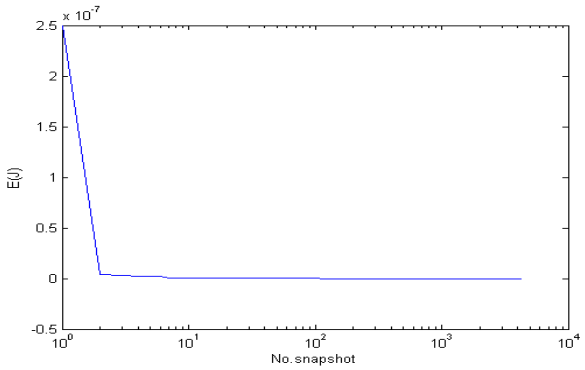

Fig.7. Snapshot to percent of abundance

The ensemble average energy of system for second helf of snap shots is drawn, and initial part is discarded. Because initial part far away to the equilibrium. diagram of energy for second helf, show that, the system reach to equilibrium.

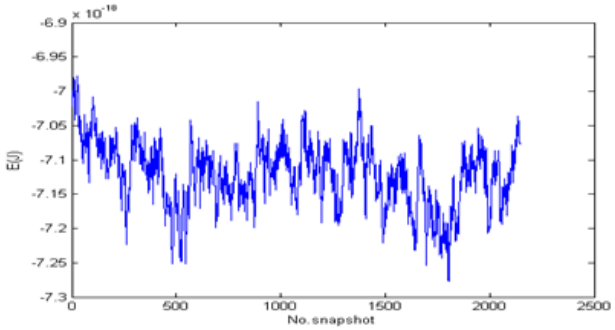

Fig. 8. .Snapshot for second helf to percent of abundance

The statistical error have been reported in this work. STDEW is the standard deviation of the calculated average in the simulation of eight number is 0.64% (simulatin error). The dimensions of simulation cell is (200 × 100 × 34.5) Å. We considered single-walled armchair (8, 8) nanotubes with open edge (Figure6).The number of carbon

atom is 320.The diameters of the nanotubes is 10.854 Å and the average bond length is 24 Å respectively. The number of molecules gas calculated by virial equation of state and input to the GCMC calculation. The equation of state of real gases is best represented, by the series (Equation 3)

$$PV_m = RT\left[1+\frac{B_{(T)}}{V_m}+\frac{C_{(T)}}{V_m^2}+\frac{D_{(T)}}{V_m^3}+\cdots\cdots\cdots\right] \quad (3)$$

Where $B_{(r)}$, $C_{(r)}$, and $D_{(r)}$ are respectively termed the second, third, and fourth virial coefficients. P is the pressure,V_m is molar volume, T the absolute temperature, and R is the gas constant[11].

$$\sigma_{ij} = (\sigma_{ii}+\sigma_{ij})/2$$

$$\varepsilon_{ij} = \sqrt{\varepsilon_{ij}\varepsilon_{jj}}$$

Table 1. *Lennard Jones* potential for interaction between gas-gas and gas-carbon nanotube

interactions	$\varepsilon_{ij}k_B^{-1}(K)$	$\sigma_{ij}(nm)$
$C_2F_6 - carbonNanotube$	83.12	3.5
$C_2F_6 - H_2$	120.43	3.6
$H_2 - carbonNanotube$	38.62	3.11
$COS - carbonNanotube$	197.3	3.43
$COS - H_2$	141.03	3.47
$CO_2 - carbonNanotube$	74.19	3.39
$H_2 - CO_2$	107.49	3.38
$CO - carbonNanotube$	50.82	3.32
$CO - H_2$	73.67	3.25
$H_2S - carbonNanotube$	92.1	3.31
$H_2S - H_2$	133.51	3.22
$NO - carbonNanotube$	57.36	3.27
$NO - H_2$	83.11	3.15
$SF_6 - carbonNanotube$	78.66	3.68
$SF_6 - H_2$	114.66	3.97
$HF - carbonNanotube$	96.46	3.27
$HF - H_2$	139.77	2.98
$CF_4 - carbonNanotube$	61.47	3.57
$CF_4 - H_2$	89.06	3.74
$SiF_4 - carbonNanotube$	69.62	3.62
$SiF_4 - H_2$	100.87	3.58

Table 2. *Lennard Jones* potential for gases

Gas	$\sigma_{ii}(nm)$	$\varepsilon_{ii}k_B^{-1}(K)$
C_2F_6	4.38	245
COS	4.13	336
CO_2	3.94	195.2
CO	3.69	91.7
H_2S	3.62	301.1
NO	3.49	116.7
SF_6	5.12	222.1
HF	3.14	330
CF_4	4.66	134
SiF_4	4.88	171.9

Table 3. *Lennard Jones* potential for interaction between hydrogen and carbon nanotube

H_2		*Carbon Nanotube*	
$\sigma_{ii}(nm)$	$\varepsilon_{ii}k_B^{-1}(K)$	$\sigma_{ii}(nm)$	$\varepsilon_{ii}k_B^{-1}(K)$
3/94	195.2	3.4	28.2

RESULT AND CONCLUSION

The first phase of research

Feasibility of separating and adsorption of oxide gases with hydrogen. In the first phase of research, adsorption of gas mixture of 50% oxide gases with 50% of hydrogen gas emissions in aluminum industry was investigated in pressure of 11 MPa and at temperature of 273.

Figures 9, 10 and 11 shows the distribution of composition of CO, CO_2 and NO gases with hudrogen, on carbon nanotubes. Potential parameters have been extracted from Ref [7].

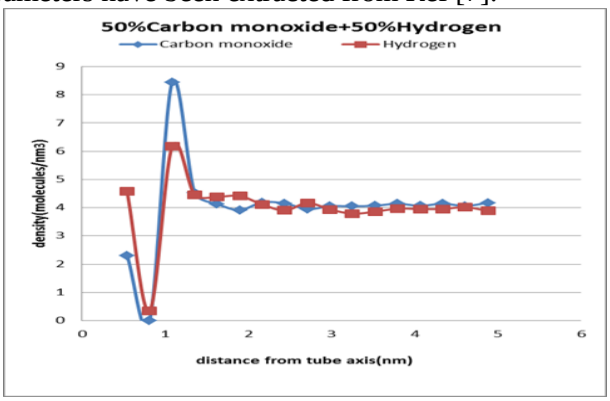

Fig. 9. Comparison of gas adsorption between carbon monoxide and hydrogen(with fifty percent combination)

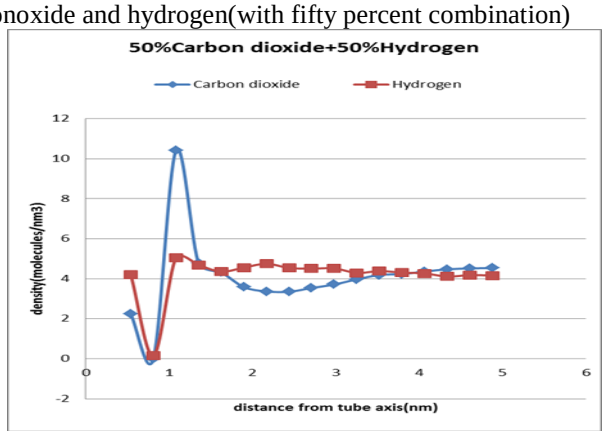

Fig. 10. Comparison of gas adsorption between carbon dioxide and hydrogen(with fifty percent combination)

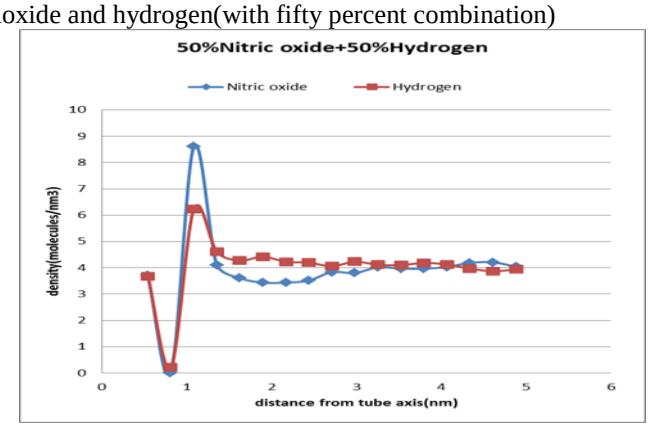

Fig. 11. Comparison of gas adsorption between nitric oxide and hydrogen(with fifty percent combination)

Considering the figure, although the number of moles of gas oxide gases and hydrogen is equal, but

the gas adsorption of oxide gases is greater than hydrogen that indicated stronger interactions between oxide gases with carbon nanotubes and according to figures, in separating, usually the diameter of nanotube, relative size of molecule and the potential of interactions are used as the most important criteria for determining the adsorption of molecules and consequently the isolation [12,13]. Since the diameter of nanotube is considered stable and is not our discussion, it seems that due to differences in relative size of molecules oxide gases and hydrogen, they are separated by a high partition coefficient.The reason for this change is that the interaction of carbon nanotube molecules and oxide gases is much more intensive than the interaction of molecules hydrogen. Therefore, the adsorption of hydrogen gas is slow.

The second phase of research

Feasibility of separating and adsorption of sulfur gases with hydrogen. In the second phase of research, adsorption of gas mixture of 50% sulfur gases with 50% of hydrogen gas emissions in aluminum industry was investigated in pressure of 11 MPa and at temperature of 273 K.

Figures(12,13,14) shows the distribution of composition of sulfur gases and hydrogen, on carbon nanotubes. Potential parameters have been extracted from Ref. [14].

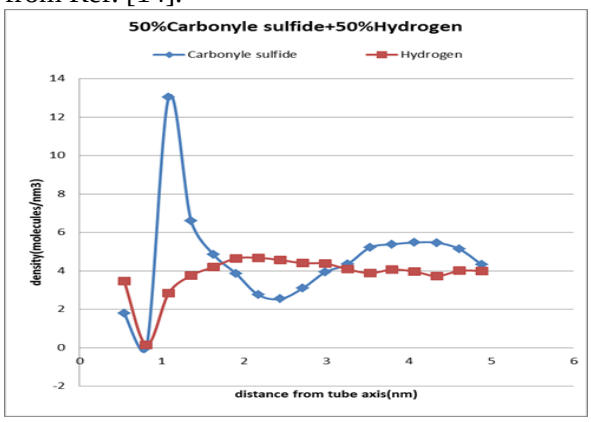

Fig. 12. Comparison of gas adsorption between 50carbonyle sulfide and hydrogen(with fifty percent combination).

Generally, internal and external walls of nanotubes can adsorb constant value of a gas.

When carbon nanotubes are filled with larger molecules of sulfur gases they have less additional sites to store small molecules of hydrogen.

According to Figures 12,13,14 related to chart adsorption of sulfur gases in combination with hydrogen in equal molar ratio show that, sulfur gases adsorption in nanotube is more than the adsorption of these gases. However, these gases show the greatest ability to adsorb in the first adsorption layer on the nanotube axis.

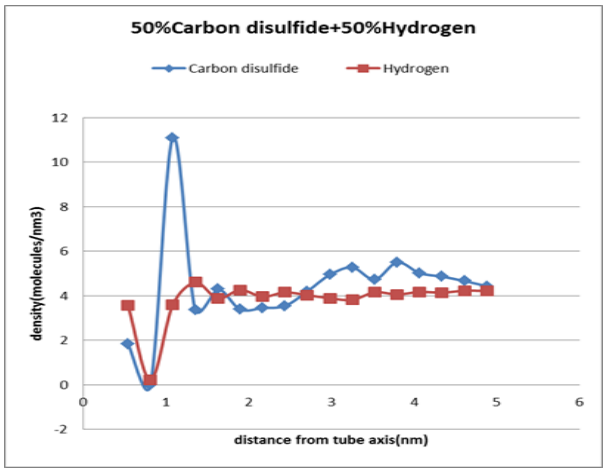

Fig. 13. Comparison of gas adsorption between carbon disulfide and hydrogen(with fifty fifty percent combination).

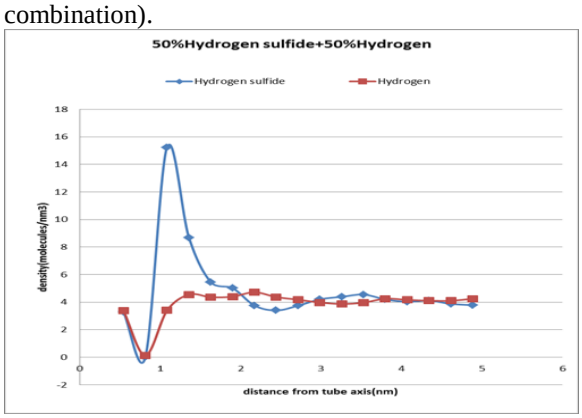

Fig. 14. Comparison of gas adsorption between hydrogen sulfide and hydrogen(with fifty percent combination)

Adsorption of combination of these gases in the second adsorbent layer is close, so their separation seems impossible. Hydrogen sulfide maximum shows more adsorption than other gases.

In this case, sulfur gases adsorption inside the nanotubes is greater similar to oxide gases. While, the maximum peak shows more adsorption and in comparison, sulfur gases shows more adsorption than hydrogen. Out of nanotubes have irregular process of adsorption. This adsorption process is opposite. So that, where hydrogen has more adsorption sulfur gases adsorb less.

The third phase of research

Feasibility of separating and adsorption of fluoride gases and hydrogen. In the third phase of research, adsorption of gas mixture of 50% fluride gases with 50% of hydrogen gas emissions in aluminum industry was investigated in pressure of 11 MPa and at temperature of 273.

Figures 15,16,17,18 shows the distribution of composition of sulfur gases and hydrogen, on carbon nanotubes. Potential parameters have been extracted from Ref. [15,16].

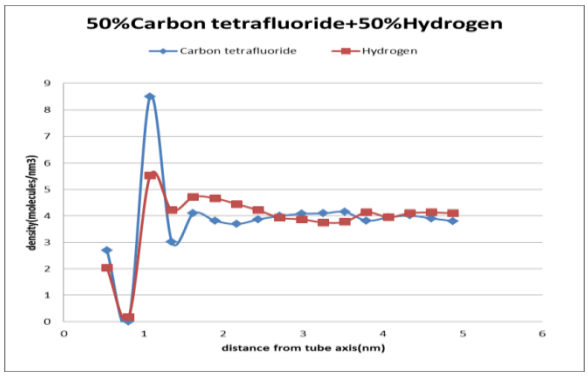

Fig. 15. Comparison of gas adsorption between carbon tetrafluoride and hydrogen (with fifty percent combination)

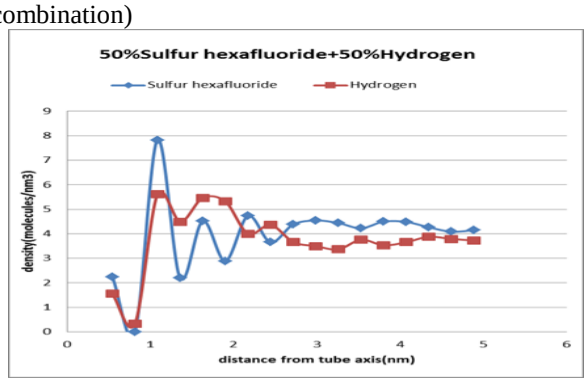

Fig. 16. Comparison of gas adsorption between sulfur hexafluoride and hydrogen(with fifty percent combination)

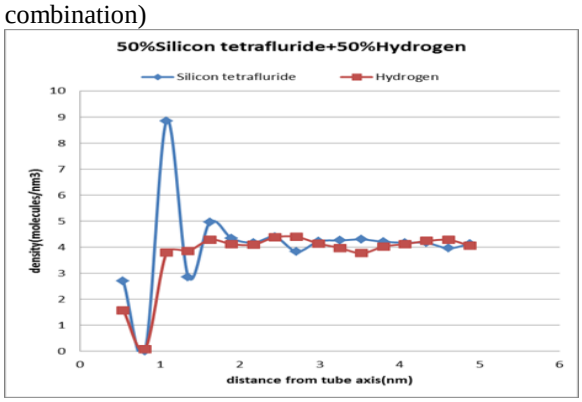

Fig. 17. Comparison of gas adsorption between silicon tetrafluride and hydrogen(with fifty percent combination).

In the case of fluoride gases, hydrogen gas adsorption is less than the respective gas inside nanotubes. Adsorption process is quite irregular from second layer in comparison with investigated oxide gases and sulfur gases. This different is completely obvious in figures. The maximum adsorption peak of hydrogen in HF gas has the highest value among studied gases.

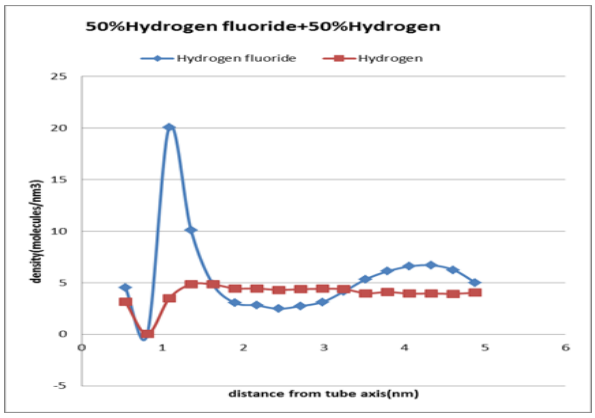

Fig. 18. Comparison of gas adsorption between hydrogen fluoride and hydrogen (with fifty percent combination)

In the following (Fig. 20 and Tables 4,5), adsorption behavior of 50% hydrogen gas was investigated in combination with 50% of other gases. Assessment of corresponding charts show that silicon tetra fluoride has lowest adsorbed density in combination with hydrogen gas. Evaluation of internal and external adsorbed density show that the highest adsorbed density is related to oxide gases.

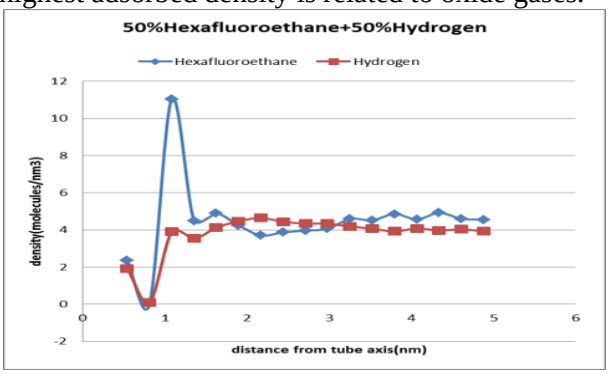

Fig. 19. Comparison of gas adsorption between hexafluoroethane and hydrogen(with fifty percent combination).

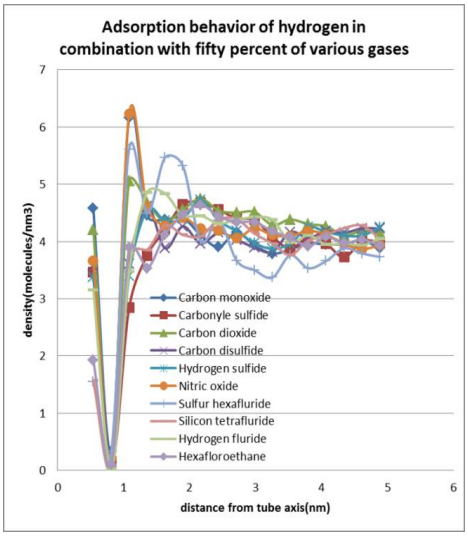

Fig. 20. Adsorption behavior of hydrogen in combination with fifty percent of various gases

Table 4, 5. The maximum adsorption peak of hydrogen gases in inside and outside of carbon nanotube

Table4		Table5	
NO	6.225661622	CO	4.577636567
CO	6.166273126	CO_2	4.203847548
SF_6	5.609881805	NO	3.663135922
CF_4	5.5242985	CS_2	3.572299245
CO_2	5.056087936	COS	3.463110147
HF	4.840584633	H_2S	3.378788297
H_2S	4.72044165	HF	3.15574205
COS	4.677454042	CF_4	2.032316801
C_2F_6	4.641359471	C_2F_6	1.923308272
CS_2	4.609606901	SiF_4	1.57067584
SiF_4	4.281876679	SF_6	1.551615368

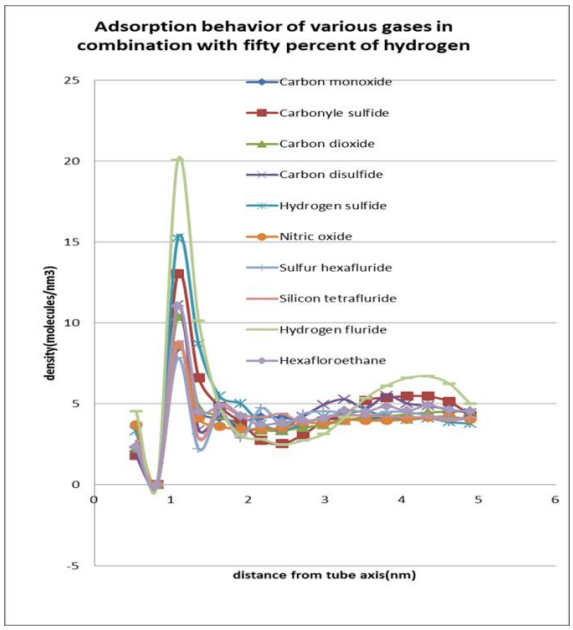

Fig. 21. Adsorption behavior of various gases in combination with fifty percent of hydrogen

In general, we investigated the adsorption behavior of 50% of each gas in combination with 50% of gas hydrogen. Adsorption behavior comparison of these gases show that the maximum adsorption peak is as follows.

In the following (Fig. 20 and Tables 6,7), adsorption behavior of 50% hydrogen gas was investigated in combination with 50% of other gases.

Table 6,7. The maximum adsorption peak of total gases in inside and outside of carbon nanotube

Table6		Table7	
HF	20.0563461	HF	4.530305765
H_2S	15.23403566	NO	3.70239685
COS	13.02971611	H_2S	3.30451561
CS_2	11.10369453	CF_4	2.698650179
C_2F_6	11.04251554	SiF_4	2.703525789
CO_2	10.41332767	C_2F_6	2.361079189
SiF_4	8.851599963	CO	2.30729476
NO	8.609230457	SF_6	2.252938157
CF_4	8.500278082	CO_2	2.23268013
CO	8.431540332	CS_2	1.852472071
SF_6	7.825949765	COS	1.802350526

Assessment of corresponding charts show that hydrogen fluoride has highest adsorbed density in combination with hydrogen gas. Evaluation of internal and external adsorbed density show that the highest adsorbed density is related to hydrogen fluoride.

Summary of adsorption behavior of these gases show that these gases have relatively similar adsorption process in composition with hydrogen gas. The highest adsorption value (adsorption peak) on the first axis of the nanotubes is as follows.

Tables 6 and 7 show the adsorption peak of these gases in combination with hydrogen. Calculations show that, Hydrogen fluoride which is one of the most important diffused gases in aluminum industry has the highest adsorption inside and outside of nanotube. After that, hydrogen sulfide indicated the greatest adsorption ability in combination with 50% hydrogen. The exact amount of other absorbance has been given in table.

Hydrogen has the highest adsorption rate in equal combination of gases such as oxide gases inside and outside of nanotubes. Exact amount of adsorption of other gases has been given in Tables 4,5.

REFERENCES

1. C. Gago, A. Romar, M. L. Ferna´ndez-Marcos, E. Alvarez, Fluoride desorption and desorption on soils located in the surroundings of an aluminium smelter in Galicia (NW Spain), Springer-Verlag Berlin Heidelberg (2014).
2. H. Mahabadipour, and H. Ghaebi, *Appl. Therm. Eng*. **50**, 771 (2013).
3. K. Sears, L. Dumée, J. Schütz, *Materials*, **3**, 132 (2010).
4. Z. Nickmand, S. F. Aghamiri, M. R. Talaie Khozanie, H. Sabzyan, *Separation Sci. Technol.*, **49**, 499 (2014).
5. S. M. Gatica, A. Nekhai, *Molecules*, **21**, 662 (2016).
6. M. Ameri, S. Ahouei, B. Bahrvand, S. Sadeghi, Applying nano-technology to remove toxic H_2S gasous compounds from exhaust gases. In: Primary Aluminium Industry, TMS, p. 57 (2013).
7. C. Draghi, A. D. Mackie, J. Bonet Avalos, *J. Chem. Phys.*, **123**, 014505 (2005).
8. Chong Gu, Guang-Hua Gao, Yang-Xin, Yu,Zong, Qinga Mao, *Int. J. Hydrogen Energy* , **26**, 691 (2001).
9. V. V. Simonyan, J. K. Johnson, *J. Alloys Compounds*, **659,** 330 (2002).
10. A. H. P Skelland, Diffusional Mass Transfer, New York: Wiley, 1985, p. 482.
11. H. Mahabadipour, H. Ghaebi, *Appl. Therm. Eng*. **50**, 771 (2013).

12. Fluoride emission management guide (FEMG), Light metals research centre, The University of Auckland, 2011.
13. E. M. Dantzler, C. M. Knobler, *J. Chem*., **73**, 1335 (1969).
14. S. Hosseini, A. Shamekhi, and A. Yazdani, *J. Renew. Sust. Ener*. **4**, 043107 (2012).
15. K. E. MacCormack, W. G. Schneider, *J. Chem. Phys*. **19**, 845 (1951)
16. A. Hamidi, and S. Jedari, *Sharif. Civ. Eng. J*. **29**, 29 (2011).